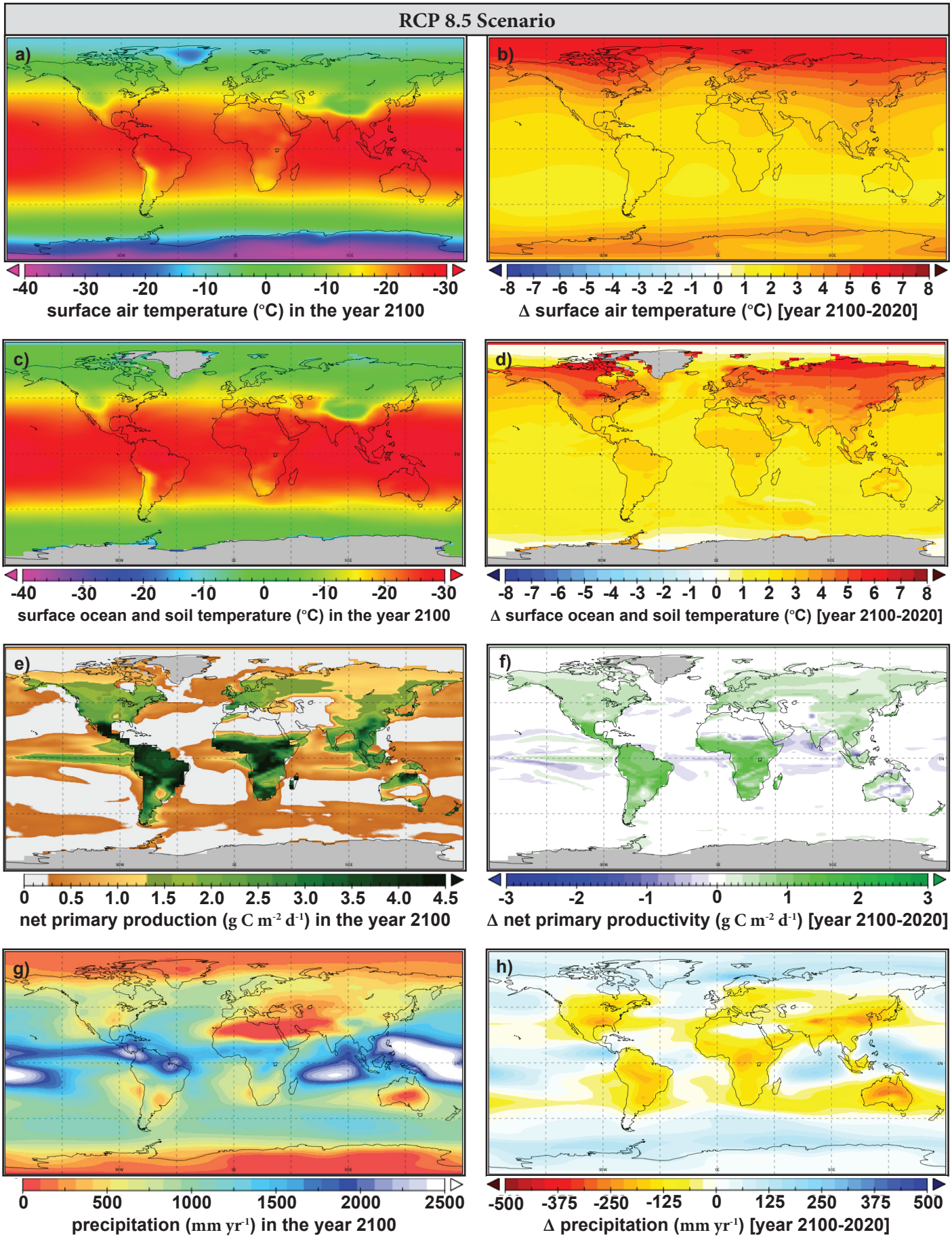


**Supplementary Figure 1 | RCP 8.5 control run simulation year 2100 properties and the change from year 2020.** The simulated control run (RCP 8.5 scenario) year 2100 mean annual surface air temperature (a), surface ocean and soil temperature (c), marine and terrestrial net primary productivity (e), and precipitation (g) and the change in each property (b, d, f, h) from the year 2020 to 2100.

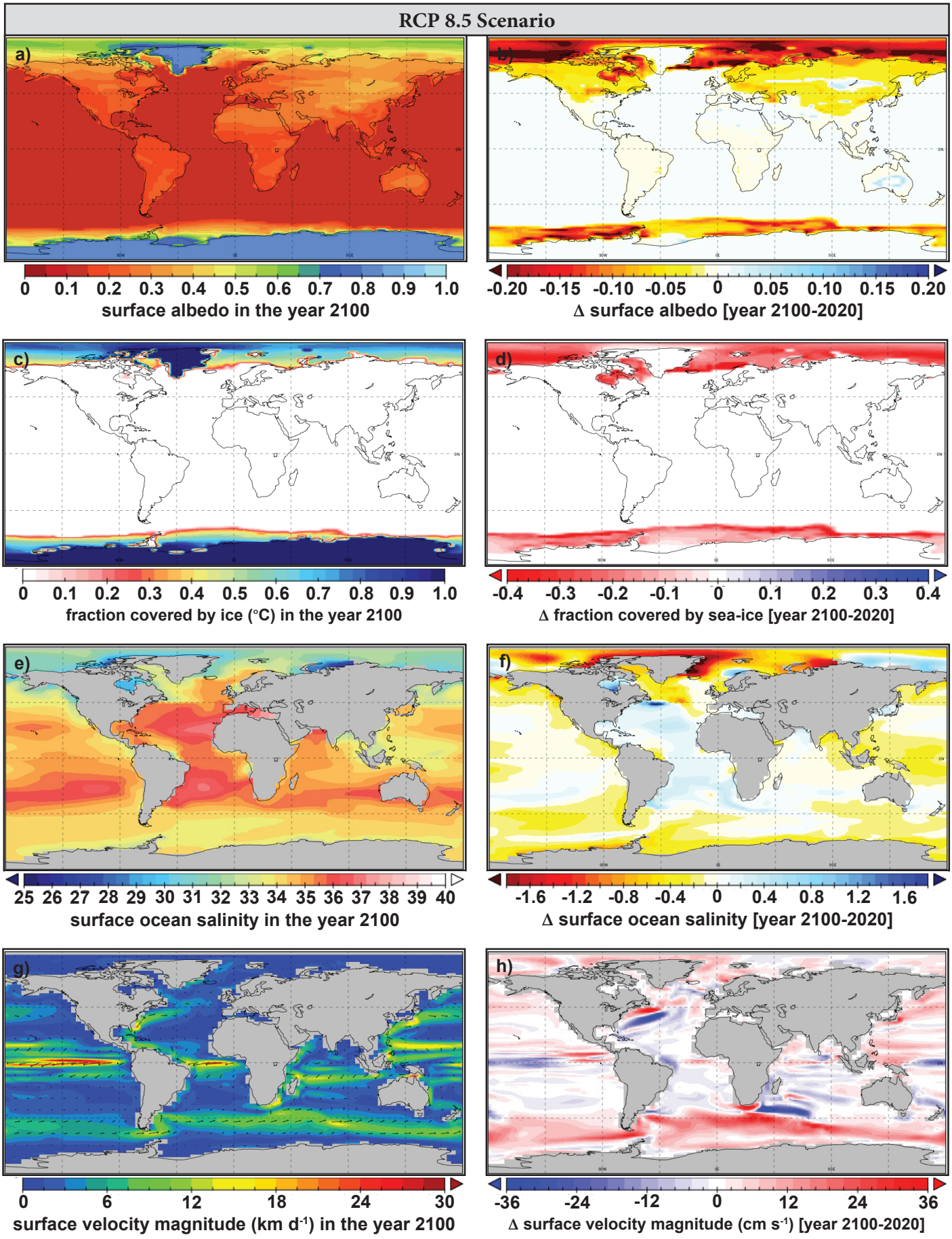


**Supplementary Figure 2 | RCP 8.5 control run simulation year 2100 properties and the change from year 2020.** The simulated control run (RCP 8.5 scenario) year 2100 mean annual surface albedo (a), fraction of each grid cell covered by sea-ice (c), surface ocean salinity (e), and surface velocity magnitude (g) and the change in each property (b, d, f, h) from the year 2020 to 2100.

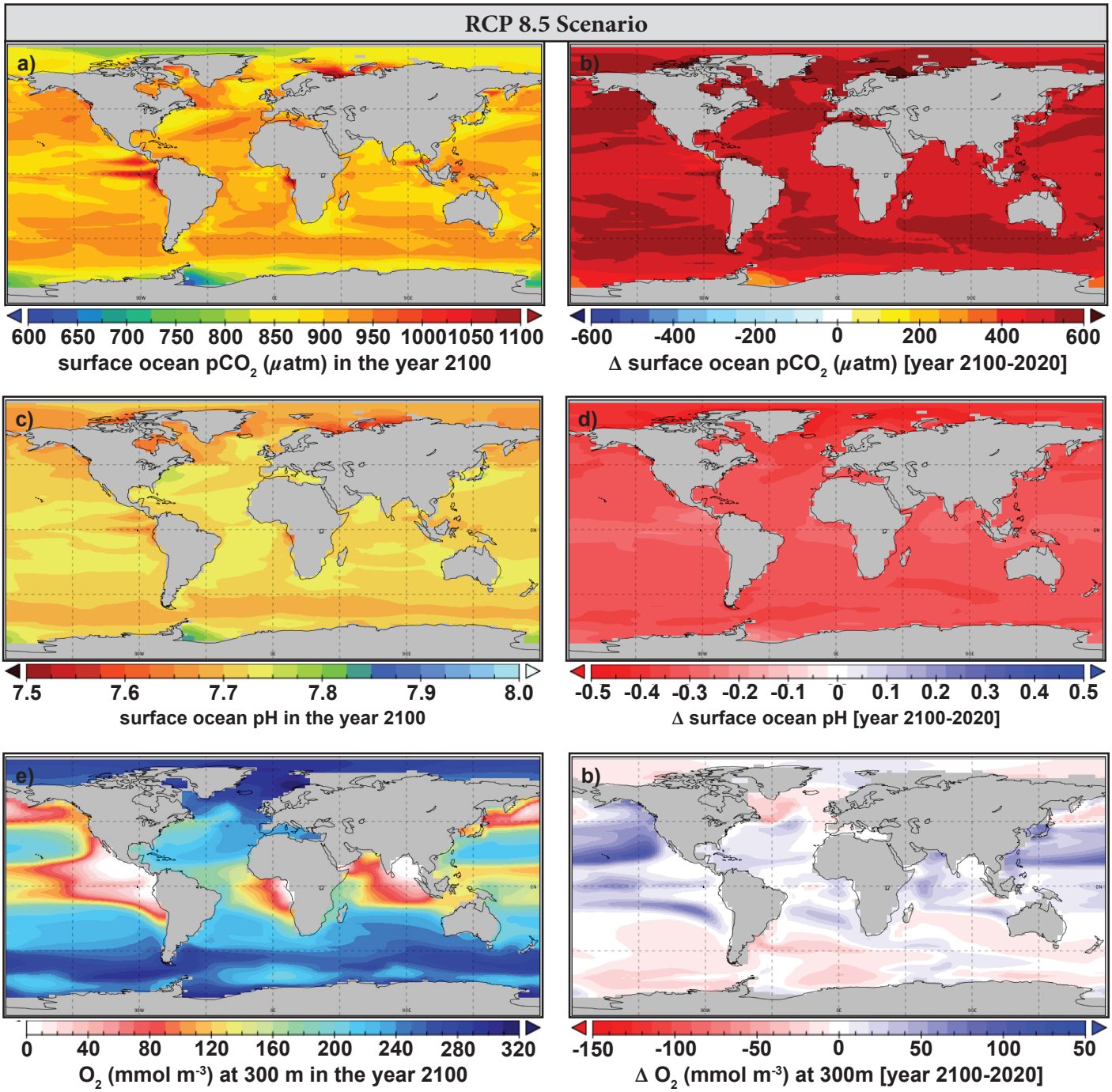


**Supplementary Figure 3 | RCP 8.5 control run simulation year 2100 properties and the change from year 2020.** The simulated control run (RCP 8.5 scenario) year 2100 mean annual surface ocean $pCO_2$ (a), surface ocean pH (c), and sub-surface ocean oxygen (e) and the change in each property (b, d, f) from the year 2020 to 2100.

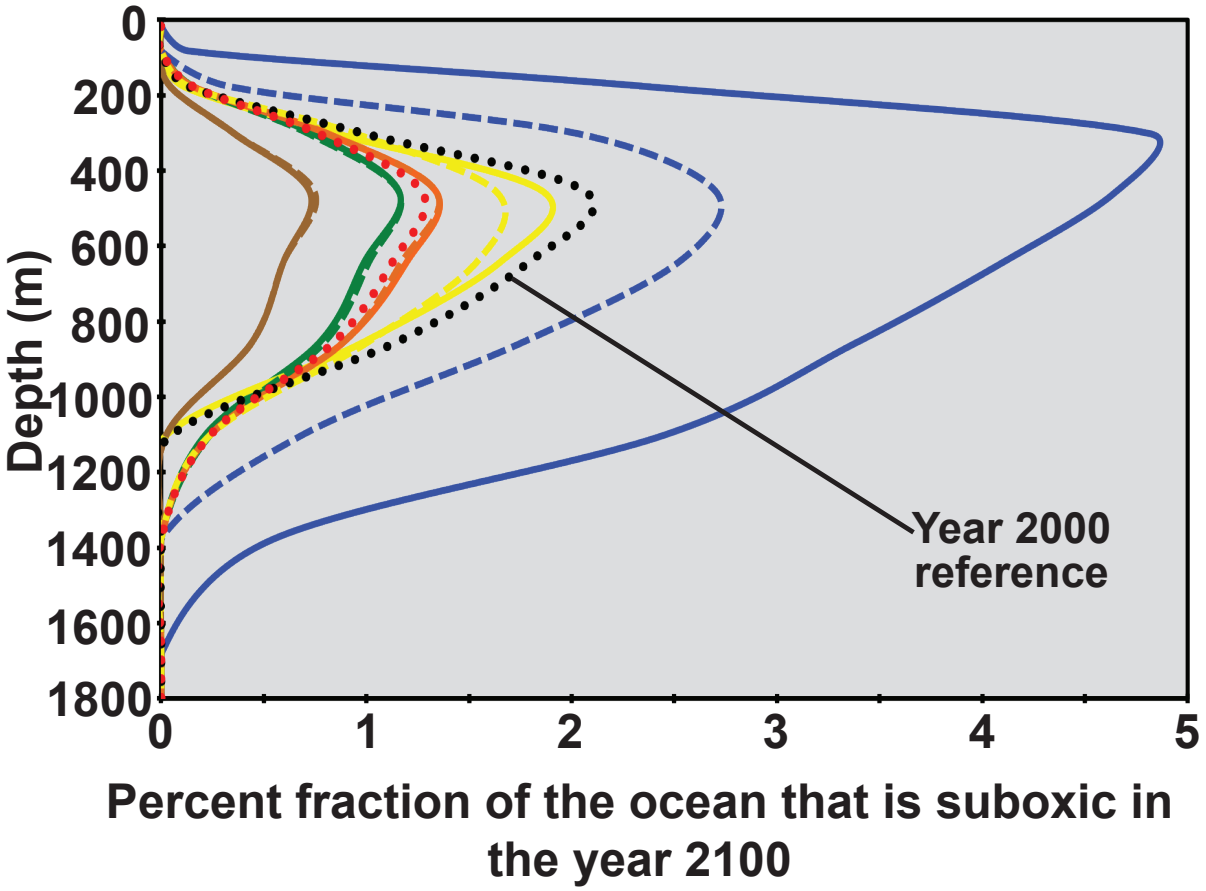


**Supplementary Figure 4 | Comparison of simulated ocean suboxic volumes.** Simulated percent fraction of the ocean that is suboxic in the year 2100 for model runs (afforestation - green; artificial ocean upwelling - blue; ocean alkalinization - orange; ocean iron fertilization - brown; solar radiation managment - yellow) where climate engineering is continuously deployed (solid lines) and runs where it was discontinued after 50 years (dashed lines). The control run, with no climate engineering (red dotted line), is also shown.

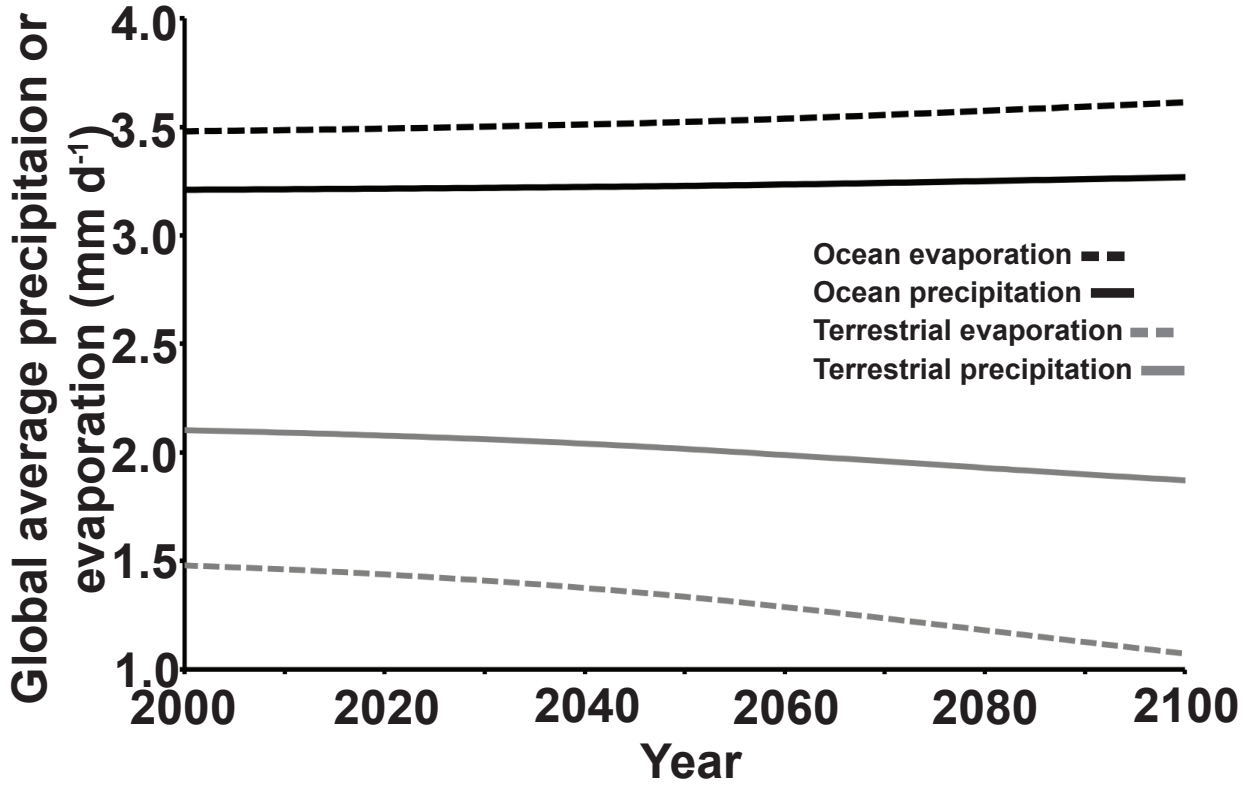


**Supplementary Figure 5 | Mean annual evaporation and precipitation in the RCP 8.5 control run.** Simulated global annual mean evaporation and precipitation over the ocean and land during the RCP 8.5 control model run.

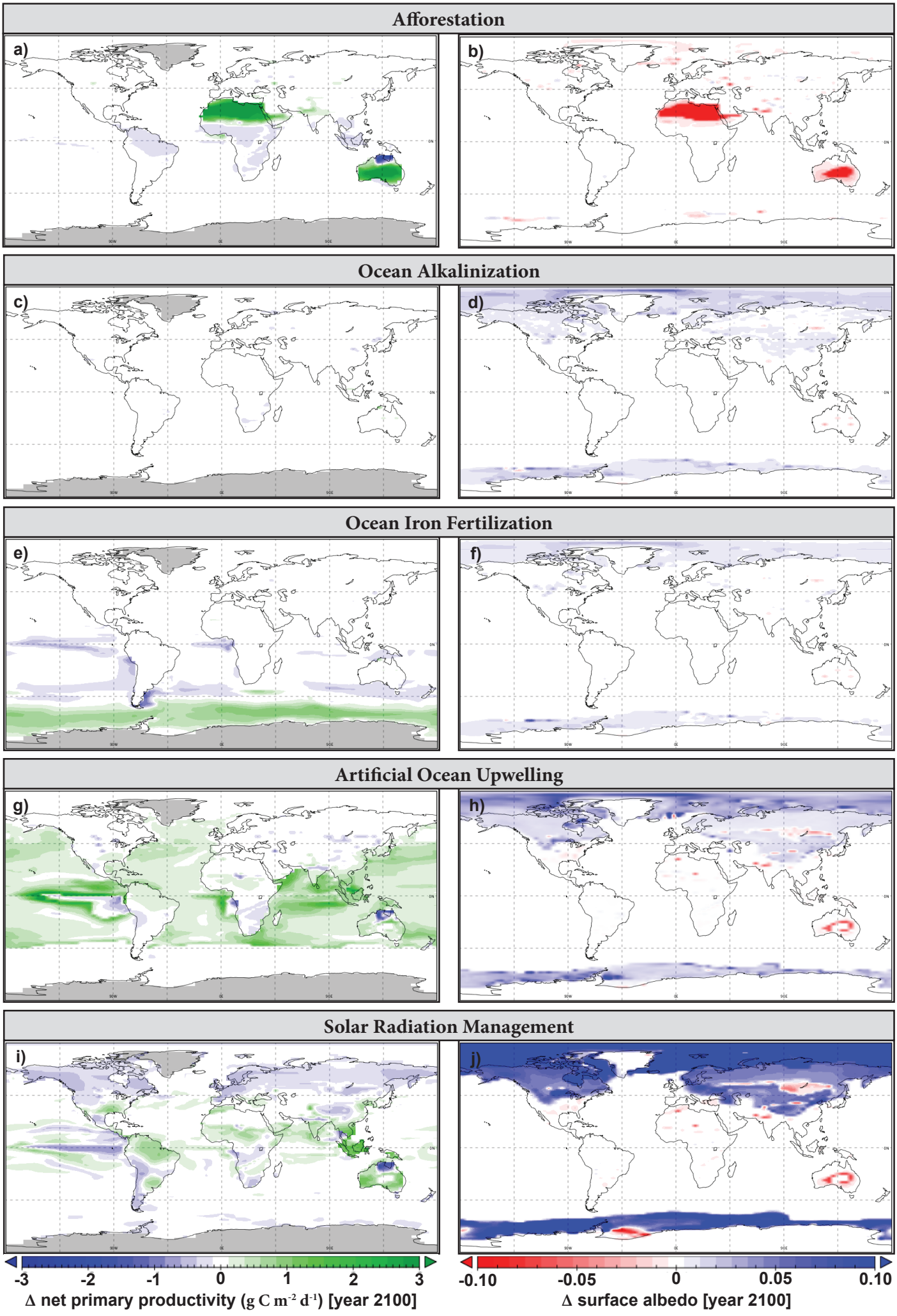


**Supplementary Figure 6 | Climate engineering method effects on primary productivity and albedo.** The simulated year 2100 mean annual differences between the climate engineering runs and the control run (climate engineering run minus the control run) for marine and terrestrial primary productivity (a, c, e, g, i) and the land and ocean surface albedo (b, d, f, h, j).

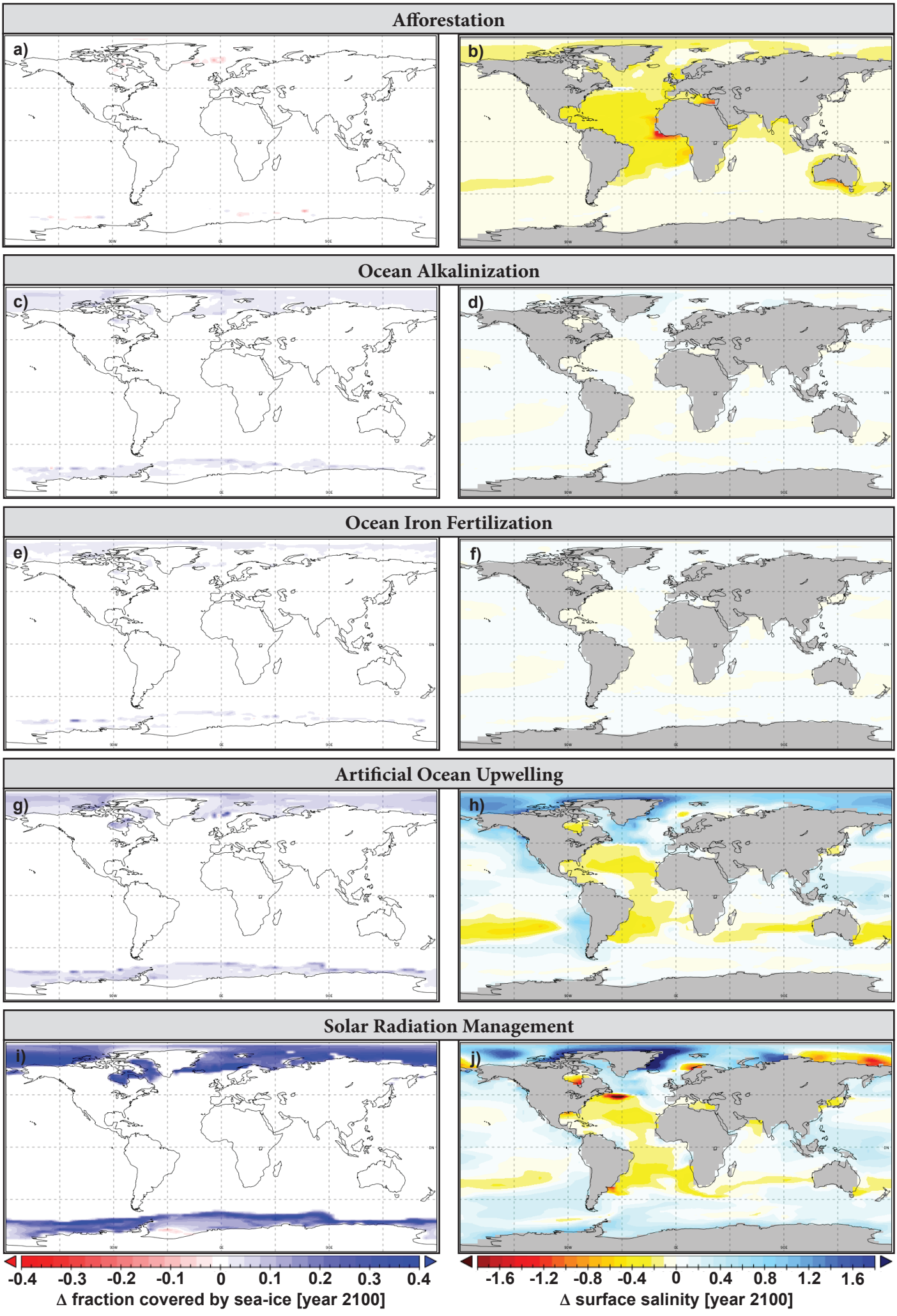


**Supplementary Figure 7 | Climate engineering method effects on sea-ice coverage and surface ocean salinity.** The simulated year 2100 mean annual differences between the climate engineering runs and the control run (climate engineering run minus the control run) for the fraction of each grid cell covered by sea-ice (a, c, e, g, i) and surface ocean salinity (b, d, f, h, j).

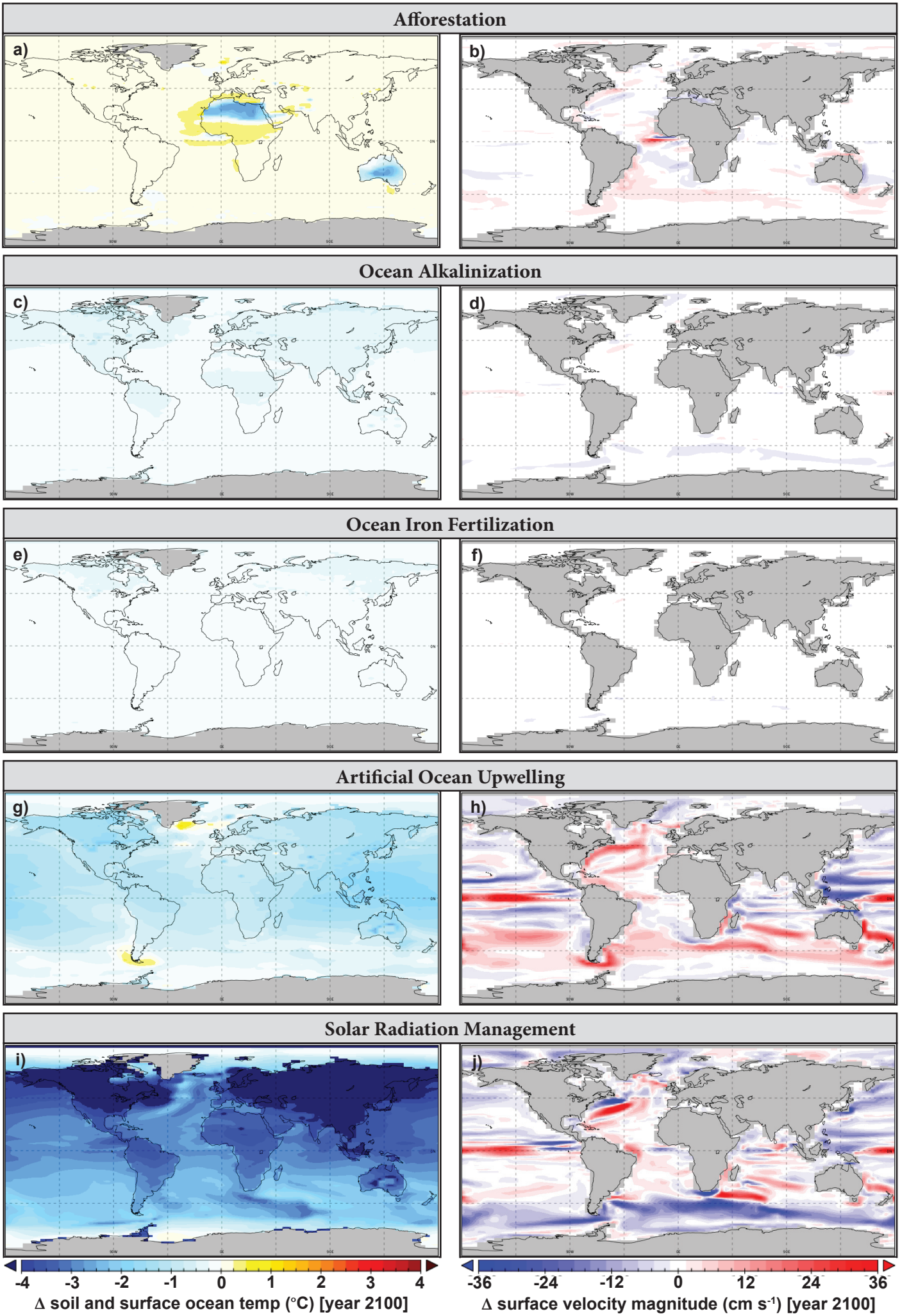


**Supplementary Figure 8 | Climate engineering method effects on surface skin temperature and ocean surface current velocities.** The simulated year 2100 mean annual differences between the climate engineering runs and the control run (climate engineering run minus the control run) for surface ocean and soil temperatures (a, c, e, g, i) and the magnitude of surface ocean velocity (b, d, f, h, j).

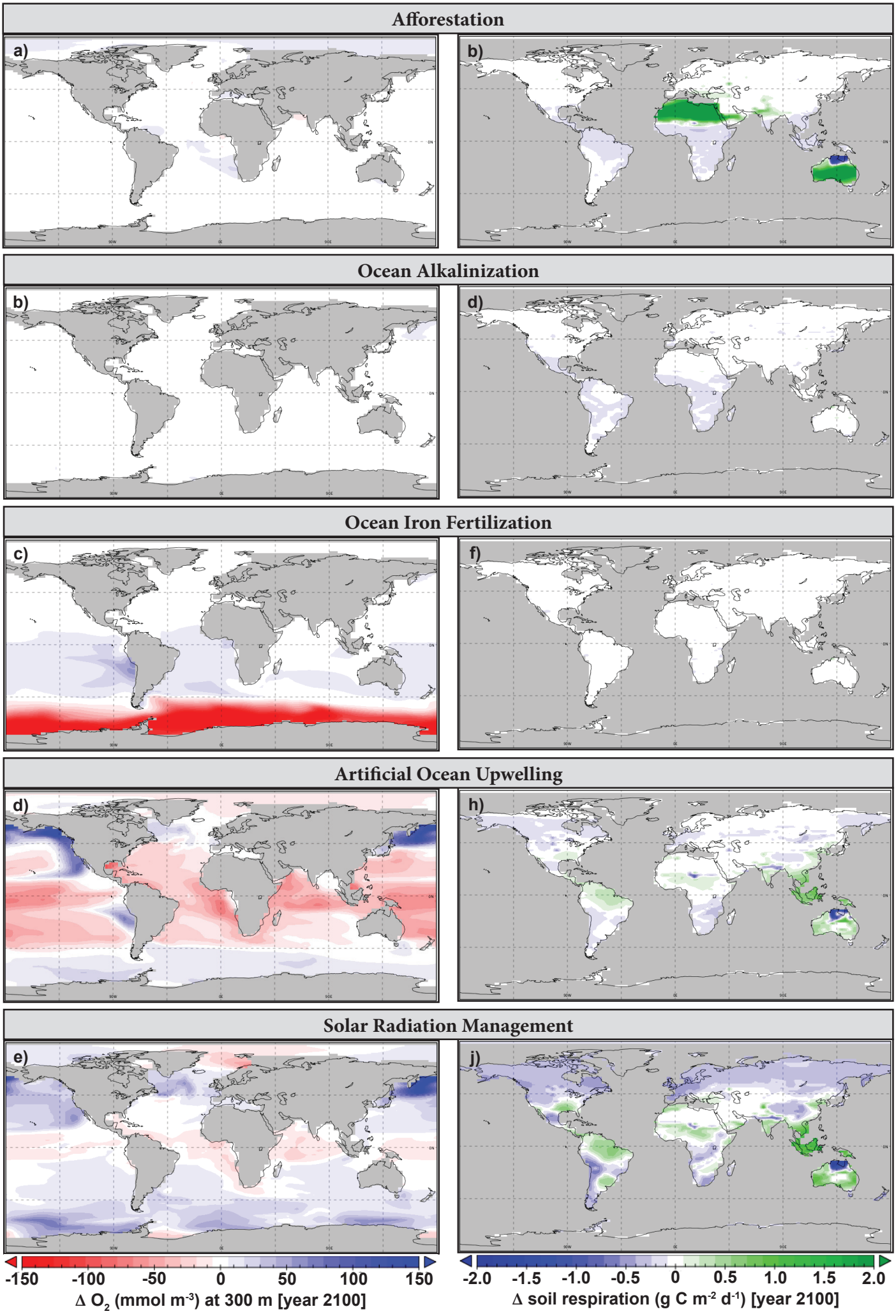


**Supplementary Figure 9 | Climate engineering method effects on sub-surface ocean oxygen and soil respiration.** The simulated year 2100 mean annual differences between the climate engineering runs and the control run (climate engineering run minus the control run) for sub-surface ocean oxygen (a, c, e, g, i) and soil respiration (b, d, f, h, j).

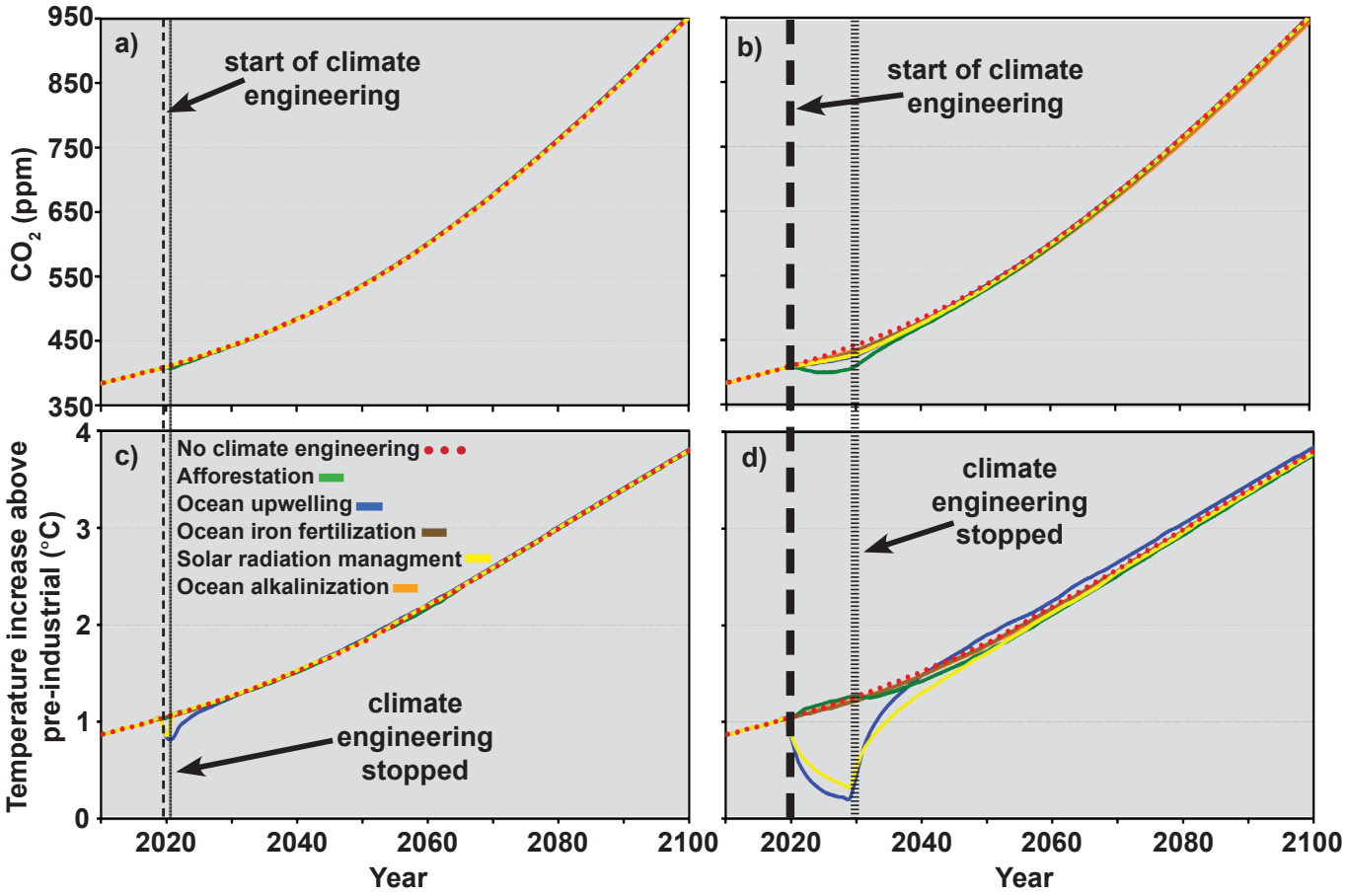


**Supplementary Figure 10 | Comparison of climate engineering method effects on temperature and $CO_2$.** Simulated changes in globally averaged annual atmospheric $CO_2$ (a, b) and surface air temperature (c, d) (relative to a pre-industrial temperature of 13.05° C) for limited duration (1 and 10 year) climate engineering simulations. The control run, with no climate engineering, is also shown.

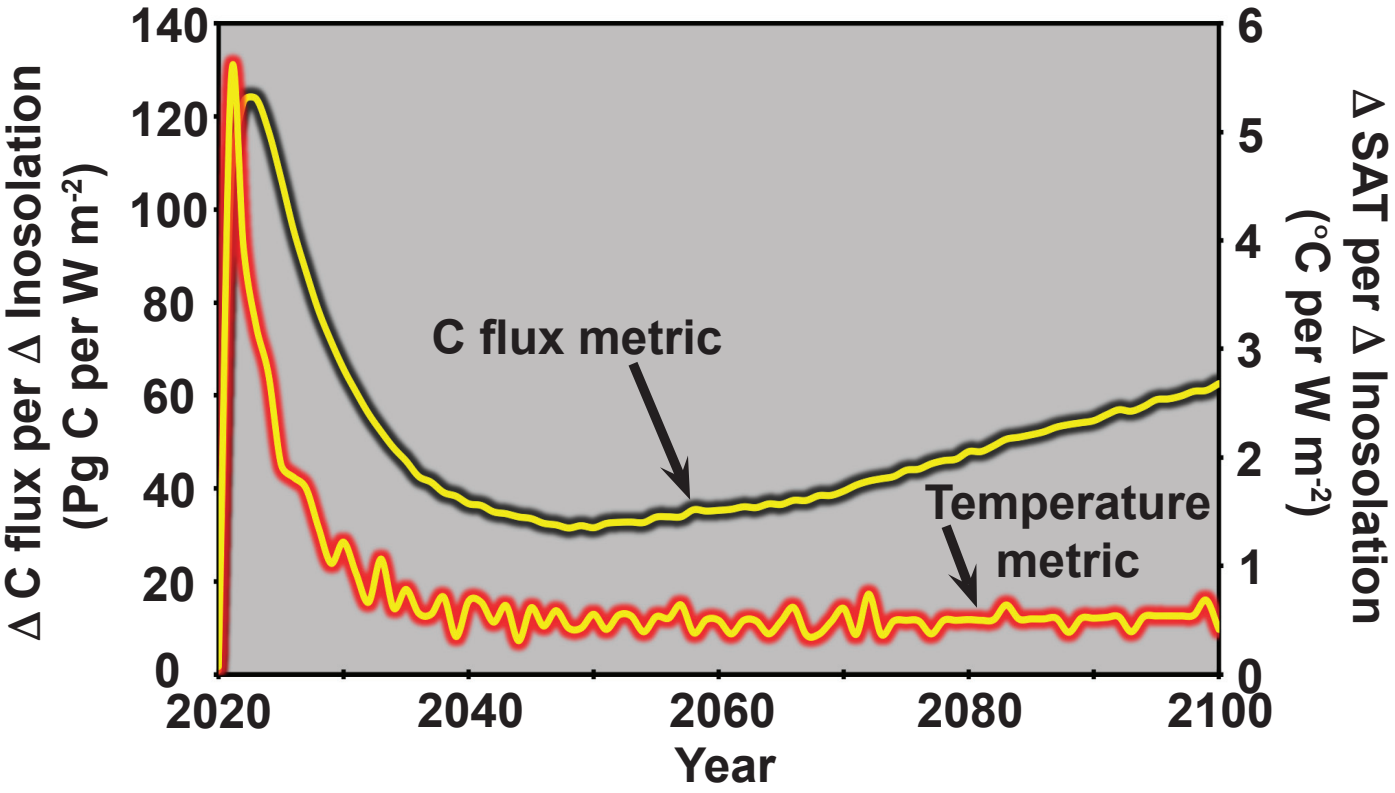


**Supplementary Figure 11 | Simulated solar radiation management efficacy.** Simulated solar radiation management (SRM) annual change in the flux of carbon from the atmosphere to the ocean or land per change in insolation and the rate of surface air temperature change (reduction) per change in insolation.

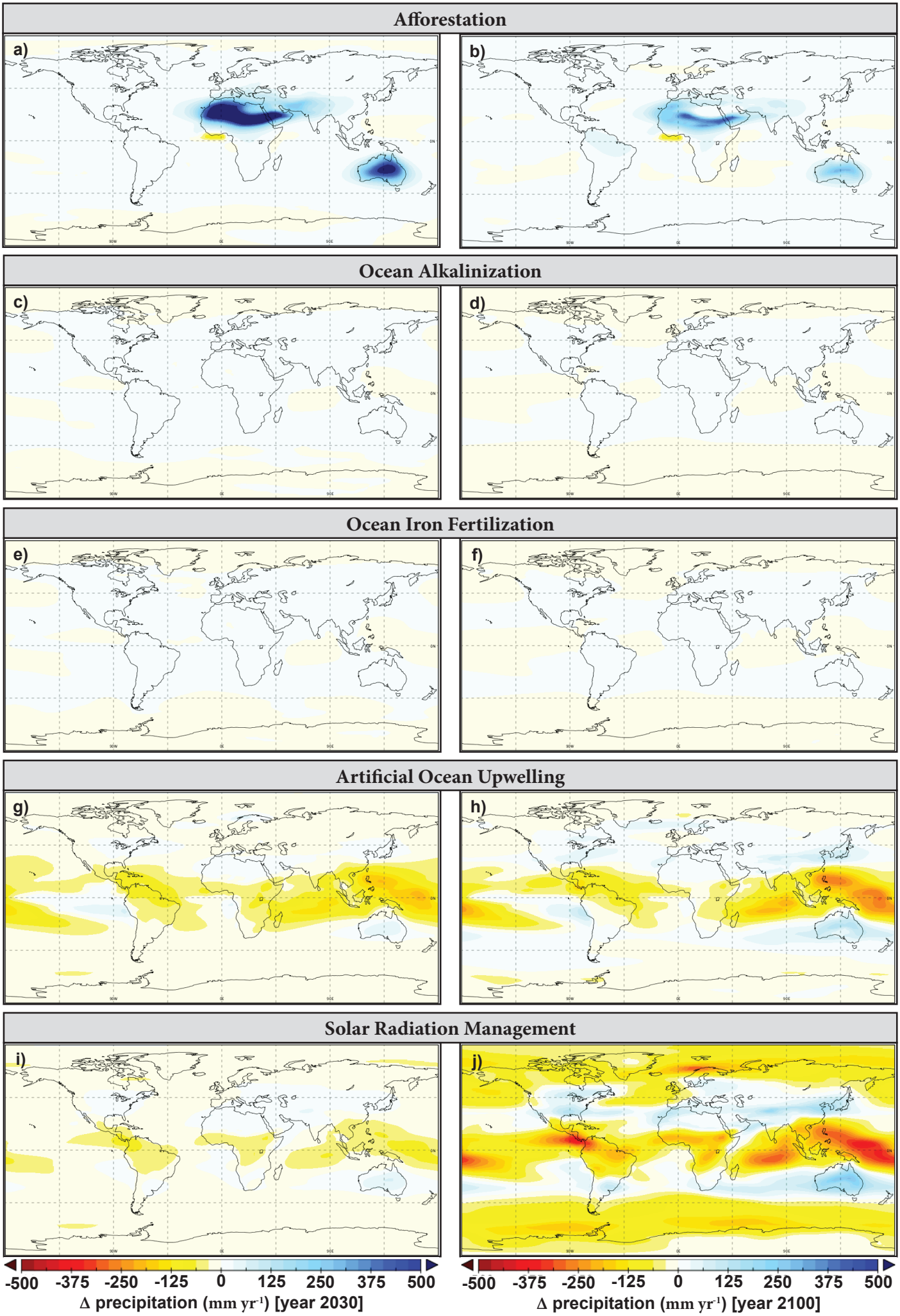


**Supplementary Figure 12 | Climate engineering method effects on precipitation.** The simulated year 2030 (a, c, e, g, i) and 2100 (b, d, f, h, j) mean annual differences between the climate engineering runs and the control run (climate engineering run minus the control run) for precipitation.

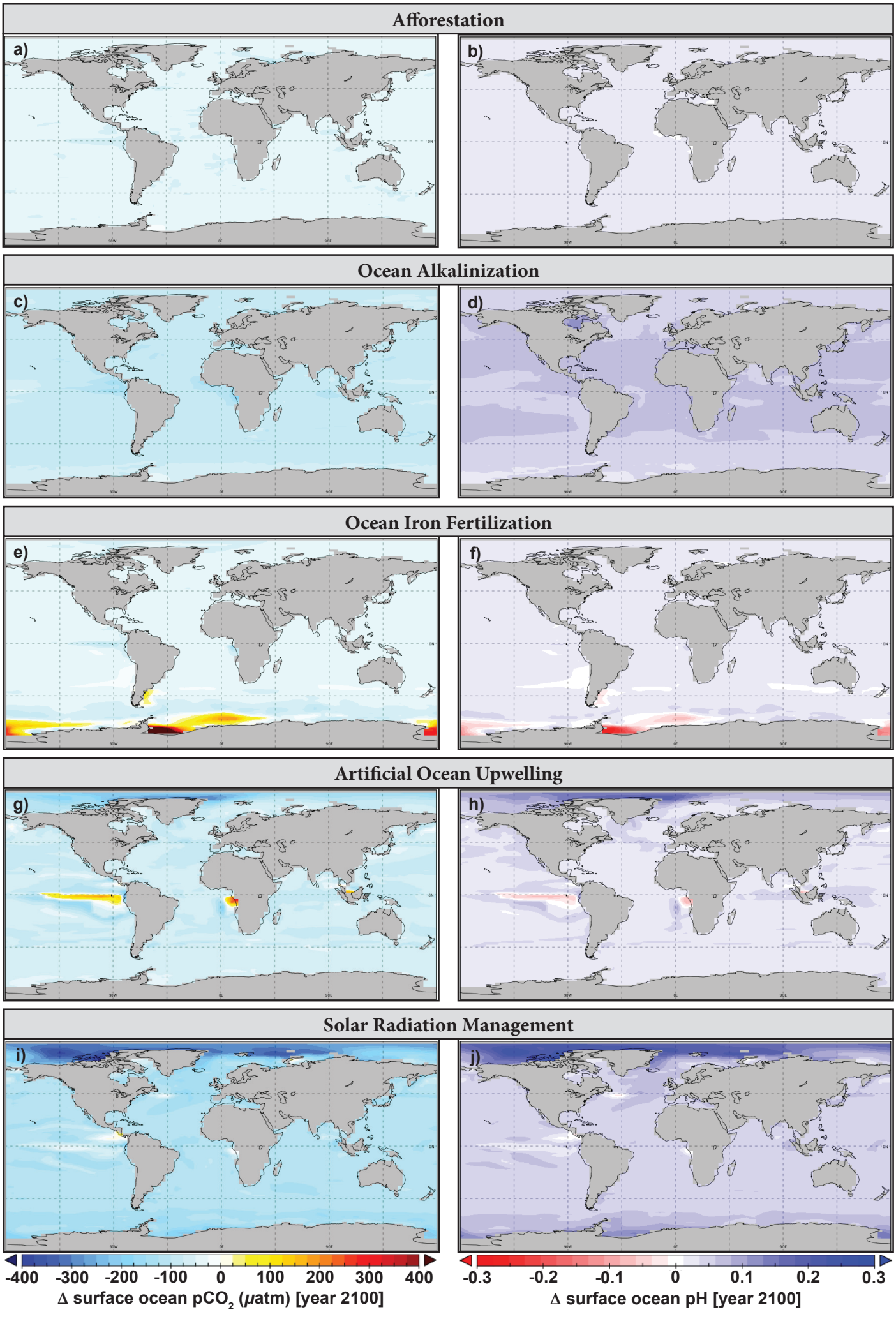


**Supplementary Figure 13 | Climate engineering method effects on surface ocean $pCO_2$ and pH.** The simulated year 2100 mean annual differences between the climate engineering runs and the control run (climate engineering run minus the control run) for surface ocean $pCO_2$ (a, c, e, g, i) and pH (b, d, f, h, j).

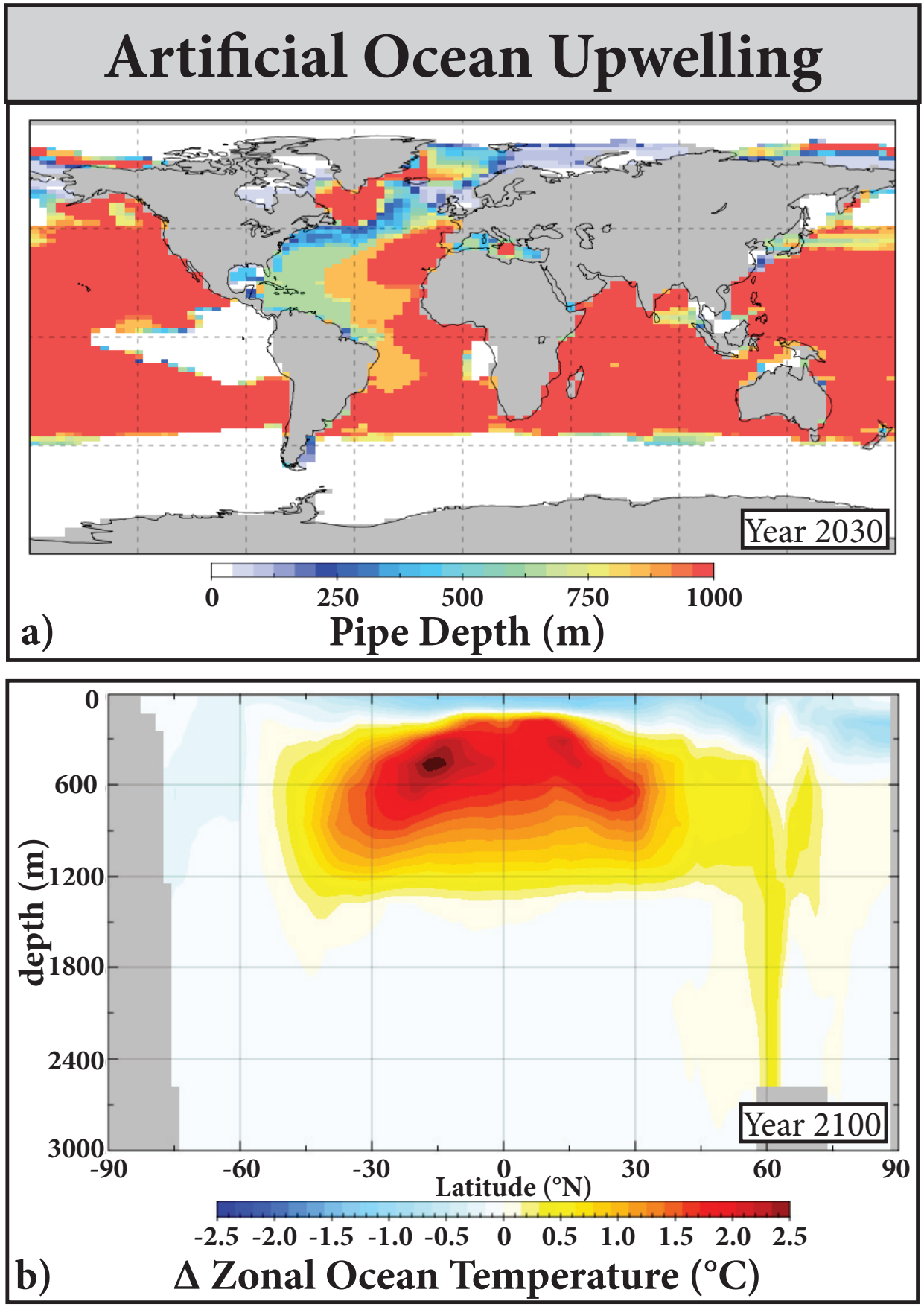


**Supplementary Figure 14 | Simulated artificial ocean upwelling pipe placement and the effects on ocean temperature.** Simulated artificial ocean upwelling pipe locations and depths (a) and the simulated year 2100 mean annual zonal ocean temperature difference (b) between the climate engineering run and the control run (climate engineering run minus the control run).

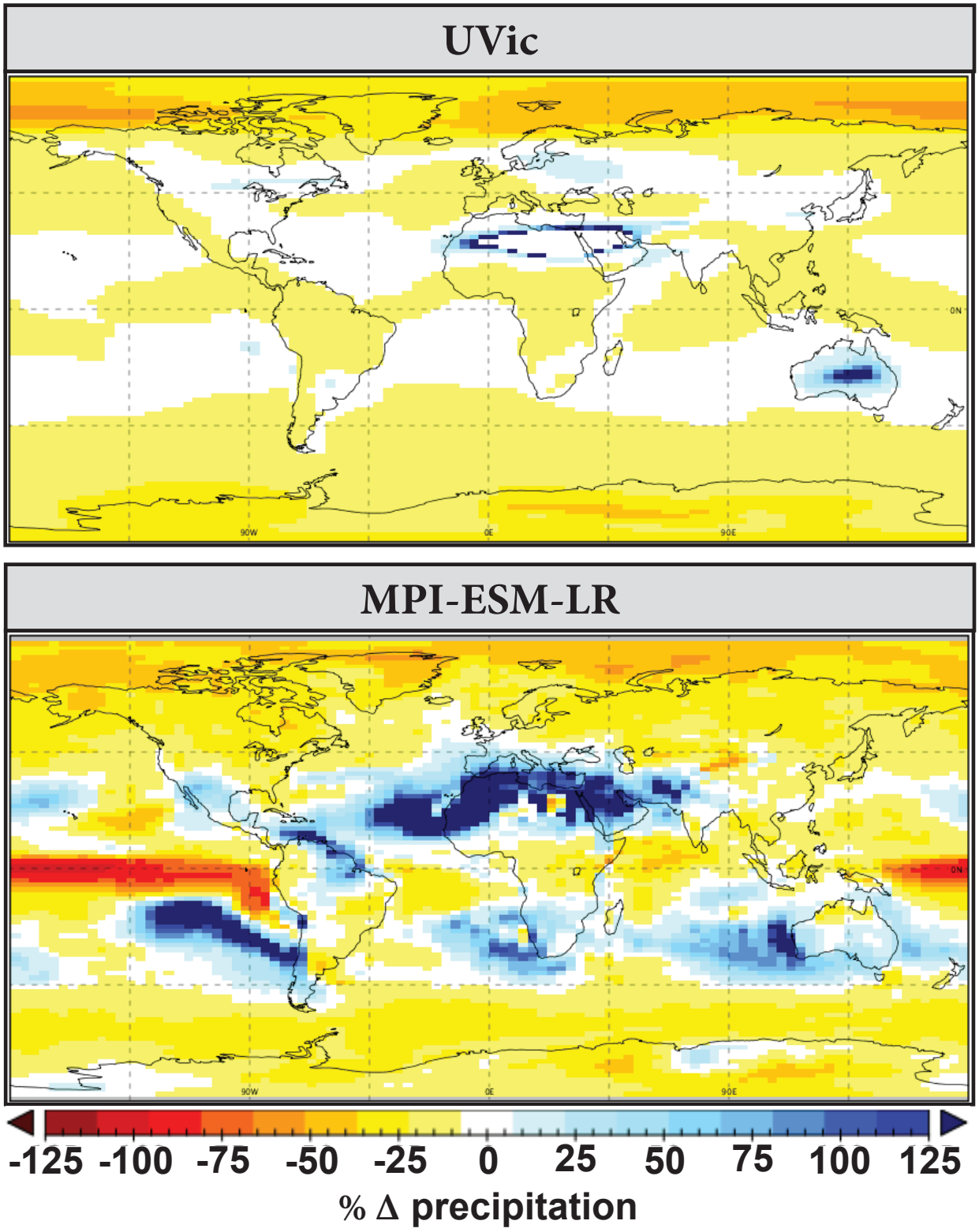


**Supplementary Figure 15 | Comparison of the change in precipitation with the UVic and MPI-ESM-LR models during GeoMIP G1 simulations.** GeoMIP G1 experiment simulated percent changes in precipitation ((G1_SRM_run –Control_run)/ Control_run), averaged over years 40-50 of the simulations. This experiment (G1_SRM_run) is conducted by instantaneously quadrupling the $CO_2$ concentration (from pre-industrial levels) while simultaneously reducing the solar constant to counteract this forcing (50 year simulation). The Control_run here for both the UVic and the MPI-ESM-LR simulations is an abrupt 4 x $CO_2$ run (from pre-industrial levels) with no SRM.

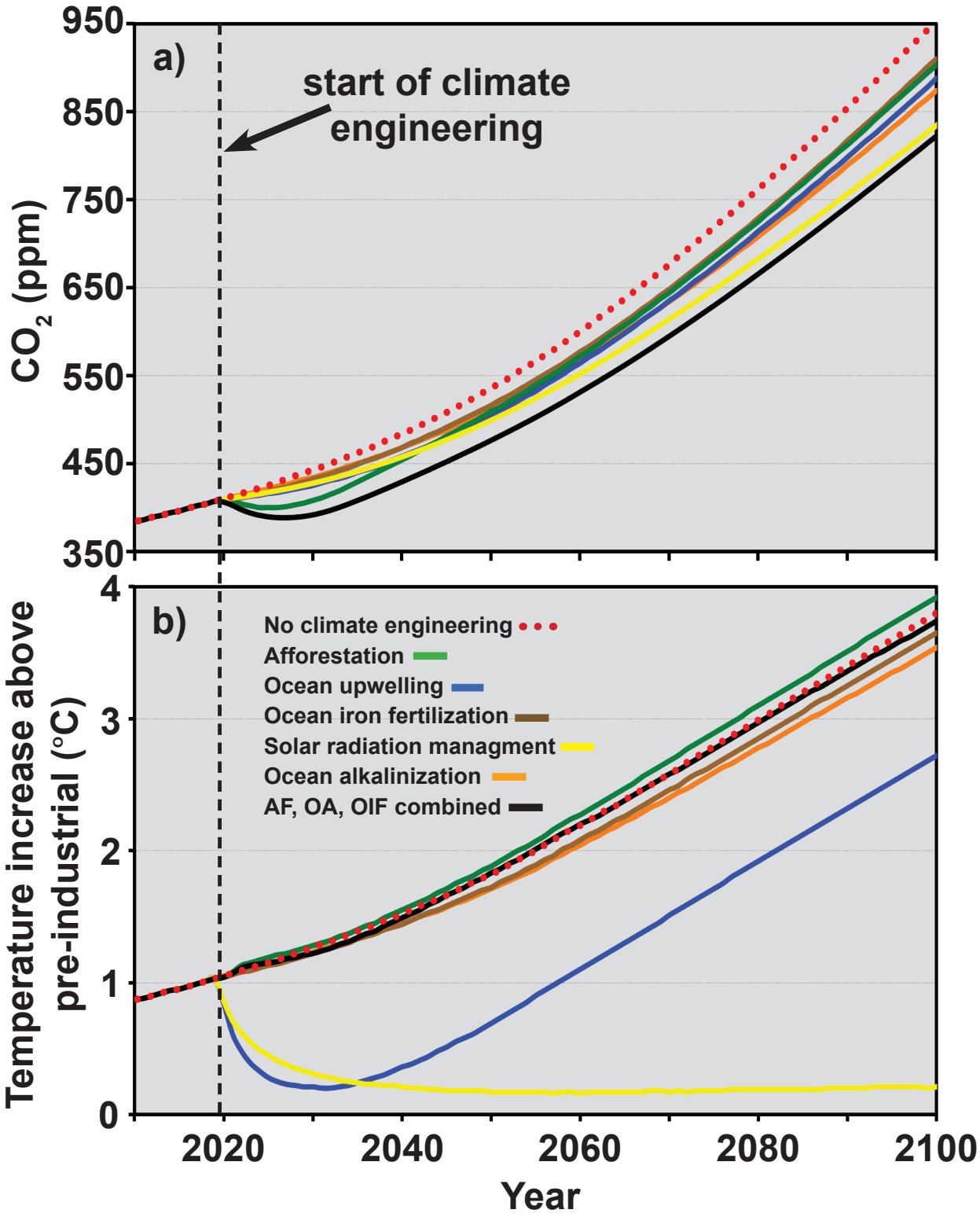


**Supplementary Figure 16 | Comparison of climate engineering method effects on temperature and $CO_2$.** Simulated changes in globally averaged annual atmospheric $CO_2$ (a) and surface air temperature (b) (relative to a pre-industrial temperature of 13.05° C) for the climate engineering simulations. The control run, with no climate engineering, is also shown.

# Afforestation

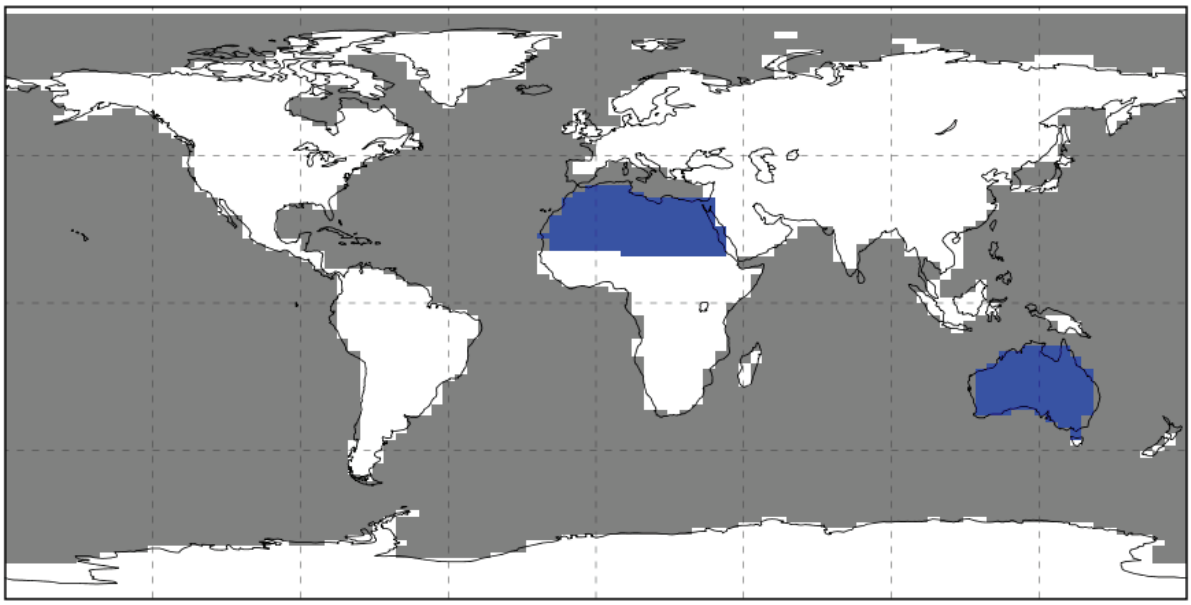

## Irrigated Region

**Supplementary Figure 17 | Simulated irrigated region for the afforestation method.**

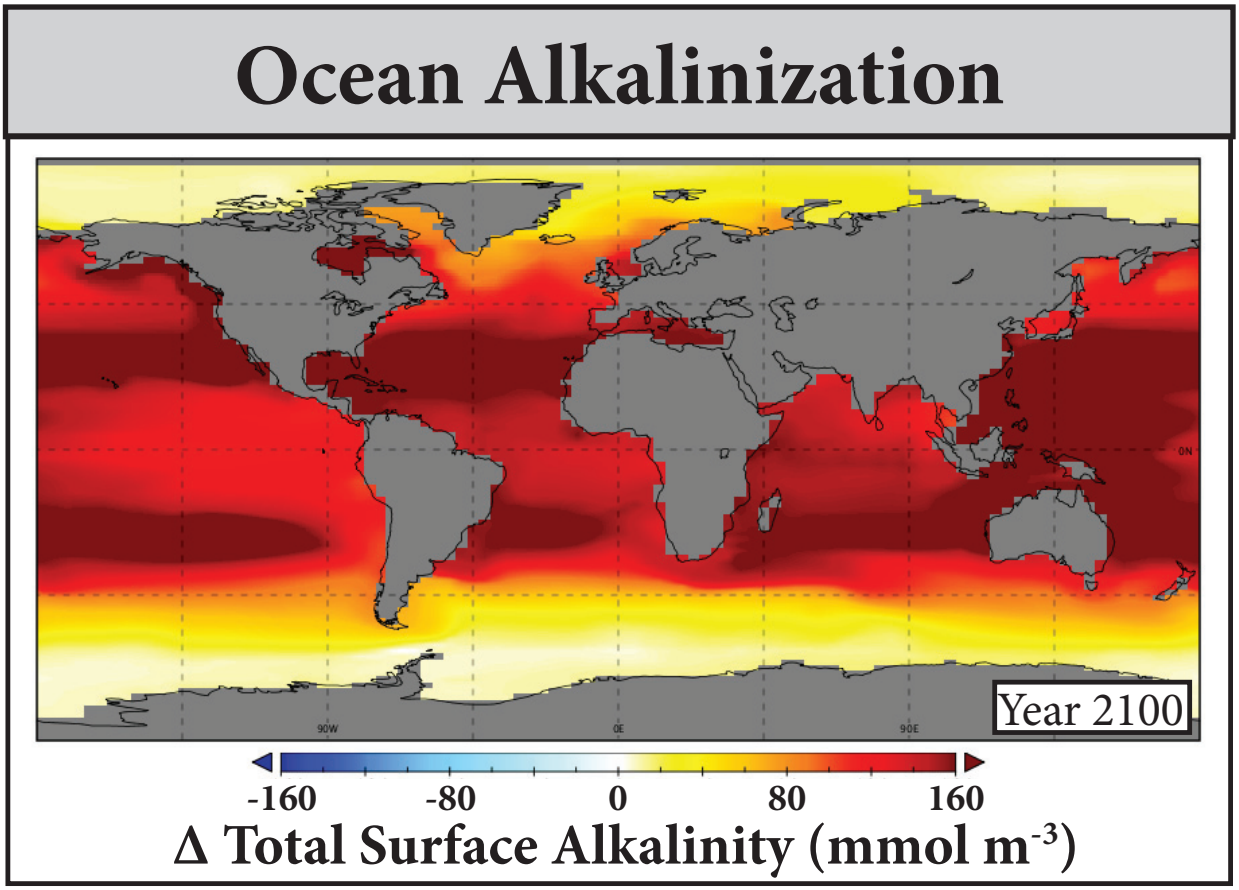


**Supplementary Figure 18 | The effects of simulated ocean alkalinization on surface ocean alkalinity.** The simulated year 2100 difference between the ocean alkalinization run and the control run for total surface ocean alkalinity.